



## Application of micro-reactor chip technique for millisecond quenching of deuterium incorporation into 70S ribosomal protein complex

Tatsuya Yamamoto<sup>a,b</sup>, Yoshihiro Shimizu<sup>c</sup>, Takuya Ueda<sup>c</sup>, Yoshitsugu Shiro<sup>d,\*</sup>, Makoto Suematsu<sup>a,b,1</sup>

<sup>a</sup> JST, ERATO, Suematsu Gas Biology Project, Tokyo 160-8582, Japan

<sup>b</sup> Department of Biochemistry, School of medicine, Keio University, Tokyo 160-8582, Japan

<sup>c</sup> Department of Medical Genome Science, Graduate School of Frontier Sciences, The University of Tokyo, 5-1-5, Kashiwanoha, Chiba 277-8562, Japan

<sup>d</sup> Biometal Science Laboratory, RIKEN SPring-8 Center, Harima Institute, 1-1-1 Kouto, Sayo, Hyogo 679-5148, Japan

### ARTICLE INFO

#### Article history:

Received 29 May 2010

Received in revised form 28 August 2010

Accepted 31 August 2010

Available online 15 September 2010

#### Keywords:

H/D exchange

Ribosome

dynamics

micro-reactor

rapid quenching

### ABSTRACT

The hydrogen/deuterium exchange (HDX) method is useful to analyze kinetics of large macromolecular complexes, although its time resolution requires further improvement. A newly developed micro-reactor chip was made of polydimethylsiloxane with a 100- $\mu\text{m}$  deep and wide microchannel. The channel in the chip has two mixing points of Y-shaped flow and allowed us to shorten time durations from the start to quenching for the HDX in 70S ribosome with high temporal resolution. This device enabled us to quench the deuterium incorporation at as early as 20 ms, detecting structural changes of individual ribosomal proteins in solution at the time scale comparable to a single reaction cycle for the peptide elongation. The profile of deuterium incorporation in individual proteins of the complex was superimposed on the X-ray crystal structure to depict the surface HDX map, revealing localization of protein movement in the ribosome. The current method serves as a useful method to visualize the regional movement of large macromolecules with high temporal resolution sufficient to examine protein dynamics.

© 2010 Elsevier B.V. All rights reserved.

### 1. Introduction

Hydrogen/deuterium exchange (HDX) study of proteins is a quantitative technique to examine protein dynamics and solvent accessibility through determining the exchange rates and ratios for the replacement of amide hydrogen with deuterium on a main chain of the protein of interests [1]. When combined with X-ray crystallography, the HDX analysis by mass spectrometry provides information of structural dynamics of proteins in solution, indicating functional movements and interactions in the macromolecular complexes. This technology thus enables us to develop new fields in protein dynamics and functional intermediates [2,3].

The *E. coli* 70S ribosome is a heterogeneous macromolecular complex (MW: 2.3 MDa) comprised of 55 proteins (these proteins are named as “S1, S2, ...” and “L1, L2, ...”) which are assembled into the complicated and asymmetric structure by noncovalent intermolecular interactions with three ribosomal RNAs (rRNA). In

previous studies, information collected by X-ray crystallography combined with cryo-electron microscopy provided evidence for structural differences in regional domains before and after the peptide elongation step [4–7]. However, such information is rather static, lacking in dynamic characterization of the movement of the domains and their spatio-temporal relationship to mechanisms for peptide elongation.

The HDX analysis supported by MALDI-TOF MS might serve as a potentially important method that overcomes the aforementioned limitation [8,9]. For rapid HDX measurements with reliable temporal resolution, several technical difficulties remain to be overcome: First, reducing amounts of individual reactants and proteins is crucial to achieve high temporal resolution. Such an approach was first performed in a previous study using multiple glass capillaries and connectors [10]. Second, reliable mixture of the reactants would be confirmed in the microreactor circuit. Finally, of great importance is accurate termination of the reaction in the circuit prior to sample transfer to MALDI-TOF MS. Taking these factors into accounts, we have herein developed a novel micro-reactor chip that made it possible to carry out accurate pulse labeling of deuterium and to achieve millisecond order of time resolution for reliable mixing and quenching the reactions, allowing us to analyze structural movement of 70S ribosome at the millisecond order in solution. The profile of deuterium incorporation into ribosomal proteins was superimposed on the X-ray crystal structure to depict the HDX surface map, revealing localization of protein movement in this

**Abbreviations:** HDX, hydrogen/deuterium exchange; MALDI, matrix-assisted laser desorption/ionization; MS, mass spectrometry; TOF, time of flight.

\* Corresponding author. 1-1-1 Kouto, Sayo, Hyogo, 679-5148, Japan.

Fax: +81 791 58 2817.

E-mail addresses: [yshiro@riken.jp](mailto:yshiro@riken.jp) (Y. Shiro),

[msuem@sc.itc.keio.ac.jp](mailto:msuem@sc.itc.keio.ac.jp) (M. Suematsu).

<sup>1</sup> Tokyo 160-8582, Japan. Fax: +81 3 5363 3466.

macromolecule ribosome at the time scale for the reaction cycle of peptide elongation.

## 2. Material and methods

### 2.1. Design of the micro-reactor chip

Micro-reactor chips have widely been utilized in device fields of chemistry to result in many advantages including down-sizing volumes of chemical reactants and shortening the reaction time. Furthermore, these methods allowed us to design the shape and length of flow path that guarantee the accurate control for starting and quenching chemical reactions as desired conditions [11].

We herein designed the micro-reactor chip as depicted in Fig. 1. Solutions mainly flow through channels with 100- $\mu\text{m}$  depth and width, mixing with different solutions at two Y-shaped channels. After passing at these mixing sites, zigzag area (2.7 nL) with a path of 50- $\mu\text{m}$  wide was placed to guarantee sufficient mixing of the samples flowing from the different paths. Such a micro-reactor chip was made of polydimethylsiloxane by Fluidware Technologies Inc., and the mixing efficiency was observed through a microscope (BX-41, OLYMPUS Corporation).

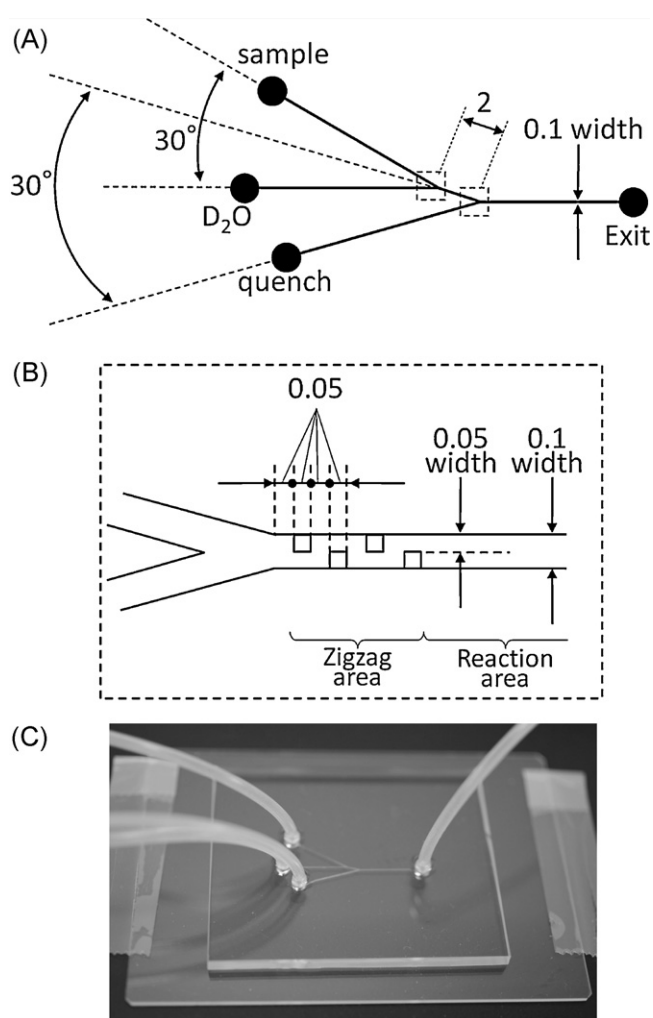


**Fig. 1.** Designed micro-reactor chip. A and B are drawings for designs of the micro-reactor chip and the mixing channel, respectively. C is an appearance picture of the micro-reactor chip. The unit of widths are mm.

### 2.2. Chemicals

Ribosome were purified from *E. coli* A19 by hydrophobic chromatography and ultracentrifugation with a sucrose cushion buffer [12], and were stored at  $-80^{\circ}\text{C}$  after resolving in 10 mM Tris buffer (pH 8.6) including 7 mM  $\beta$ -mercaptoethanol and 10 mM magnesium acetate.  $\text{D}_2\text{O}$  (99.9% atomic D) and acetic acid-*d* (99% atomic D) were purchased from EURISO-TOP and IsoTec, respectively. All other chemicals were of analytical grade.

### 2.3. Normal quenching of HDX

Deuterium incorporation was initiated by mixing 90  $\mu\text{L}$  of  $\text{D}_2\text{O}$  with 9  $\mu\text{L}$  aliquots of approximately 10  $\mu\text{M}$  ribosome solution in 1.5-mL centrifuge tubes at  $22^{\circ}\text{C}$ ; the H:D atomic ratio was 1:10. The pH of mixture in reaction was 7.1–7.2, and the  $\text{Mg}^{2+}$  concentration was prepared as 5 mM. After 20, 60, 600, 1200, and 12000 seconds, 5  $\mu\text{L}$  of the reaction mixture was removed, and the exchange reaction was quenched by adding 2  $\mu\text{L}$  of 10% acetic acid (H:D = 1:10, pH 2.9) and freezing with liquid nitrogen. The HDX experiment for 200 min was a separate experiment using similar methods in previous studies [8,9].

### 2.4. Rapid quenching of HDX

Deuterium incorporation was initiated by mixing  $\text{D}_2\text{O}$  solution with ribosome solution at  $22^{\circ}\text{C}$  in a designed micro-reactor chip; the H:D atomic ratio was 1:10. After 20 and 148 milliseconds, the reaction mixture was substantially quenched by mixing with 10% acetic acid (H:D = 1:10, pH 2.9); the reaction solution: acetic acid ratio was 5: 2. About 7  $\mu\text{L}$  of substantial quenched solutions were frozen with liquid nitrogen. All solutions were flowed in micro-reactor by syringe pumps (Model 11 plus and PHD2000, HARVARD).

### 2.5. Mass spectrometry

A portion of quenched solution was mixed with 10 mg/mL 3,5-dimethoxy-4-hydroxycinnamic acid in 70% acetonitrile containing 0.2% trifluoroacetic acid, and loaded on the sample plate for MALDI. At three minutes after loading the sample plate under a pressure of 7 Pa, the plate was set up for MALDI-TOF mass spectrometer at  $10^{-4}$  Pa.

All mass spectra were measured using MALDI-TOF mass spectrometer (Voyager DE-PRO, Applied Biosystems). Peaks were identified in a previous study [8], and overlapped peaks were deconvoluted to each peak as Gaussian type by the graph software. The spectrum was distributed over a wide range of masses, and hence was calibrated by separating into six regions: 3000–7000, 7000–11000, 11000–15000, 15000–20000, 20000–25000, and 25000–32000  $m/z$ . The spectra of deuterated ribosomes showed similar peak patterns, and it was possible to detect 52 peak shifts associated with HDX. Thus, we could use MS to successfully analyze deuterium incorporation of 52 ribosomal proteins.

### 2.6. Analysis

All masses were read from the centroid values of each peak. Deuterium incorporation,  $D$ , was calculated by the following equation:

$$D = (M_t - M_{\text{side}}) / (M_{100\%} - M_{\text{side}})$$

Where  $M_t$  is the mass of each protein after exposed time ( $t$ ) to  $\text{D}_2\text{O}$  from starting H/D exchange.  $M_{100\%}$  and  $M_{\text{side}}$  are fully deuterated masses of all residues and side chains only, respectively, at H:D = 1:10. Then, the exchange of side-chain protons is completely

terminated by acid quenching. H/D exchange was carried out three times at each quenching time, and deuterium incorporation show the average. In this experiment, errors of incorporation into each protein were  $<0.05$ . The back exchange of H for D was calculated as  $<0.03\%$  using 100% deuterated melittin.

### 3. Results and discussion

#### 3.1. Performance of the micro-reactor chip

The performance of the newly developed micro-reactor chip was examined by direct observation of the liquid interface between 1 mg/ml ribonuclease A and  $D_2O$  through microscopy. Proteins contacted with  $D_2O$  from another path in the first Y-shaped channel. These solutions gradually mixed through the turbulent flow in zigzag area, which have a narrower path of 50- $\mu\text{m}$  wide. When the incompletely-mixed solution was transferred to the downstream reaction area with 100- $\mu\text{m}$  width, protein molecules were mixed with  $D_2O$  completely through the diffusion effect. After short duration for HDX, the deuterium incorporation substantially was quenched by acetic acid at the second mixing channel with the same shape.

The duration of the HDX reaction in the present chip system was determined by the flow rate in the reaction area, although faster solution sending generally generates immiscible state by laminar flow. To explore the minimum reaction time with an enough mixing efficiency, protein and  $D_2O$  were pumped into reaction area at various flow rates, observing liquid-liquid interfaces (Fig. 2). At 880  $\mu\text{L}/\text{min}$ ,  $D_2O$  and protein kept the immiscible state at the quenching point, although the reaction solution was turbulent. The examination at 220  $\mu\text{L}/\text{min}$  also showed a clear line (laminar flow) of the interface between solutions. On the other hand, the line disappeared with the enough efficiency at 110 and 2.53  $\mu\text{L}/\text{min}$ . Finally, HDX of ribosome complexes was examined at 55  $\mu\text{L}/\text{min}$  ( $D_2O$ : 50  $\mu\text{L}/\text{min}$ , and protein solution: 5  $\mu\text{L}/\text{min}$ ), which is a half of 110  $\mu\text{L}/\text{min}$ . The exchange time was defined as 20.1 ms from this flow rate. Then, because mixed and unmixed samples exist in zigzag area, this chip system allows us to define the transit time as mixing error which is  $\pm 2.7$  ms. In this case, the chip system guarantees the accurate quenching through the following methods; Syringe pumps sent substantial quenched proteins from the second mixing channel to the exit in 1 s. A part of the sample was taken from the stream and quenched deuteration completely by freezing with liquid nitrogen.

#### 3.2. Deuterium incorporation in ribosome

To monitor peak shifts of each protein by deuterium incorporation, the base spectrum of the undeuterated ribosome was measured under the same conditions as in the HDX experiments (Fig. 3). Ionized ribosome particles by MALDI were separated into protein and rRNA components, using positive ion mode in the range of 3,000–32,000  $m/z$ ; therefore, their peaks correspond to ribosomal proteins and are not negatively charged rRNAs. We succeeded in observing analyzable peaks of 52 ribosomal proteins from this spectrum. When ribosomes contacted with  $D_2O$  for 20 ms in micro-reactor, all protein peaks shifted to higher  $m/z$ . The inset in Fig. 3 shows peak shifts of typical S5 protein, the peak of which at 20 ms indicated lower and wider  $m/z$  than 200 min. A dispersed peak in HDX spectra generally means that the protein incorporates deuterium at various ratios, which comes from the number of more stable conformations than the detection time. Fig. 4 showed time courses of HDX by calculated deuterium incorporations from peak shifts of 52 proteins. The observation time was in a range between 20 ms and 200 min as indicated by logarithmic scale for x-axis.

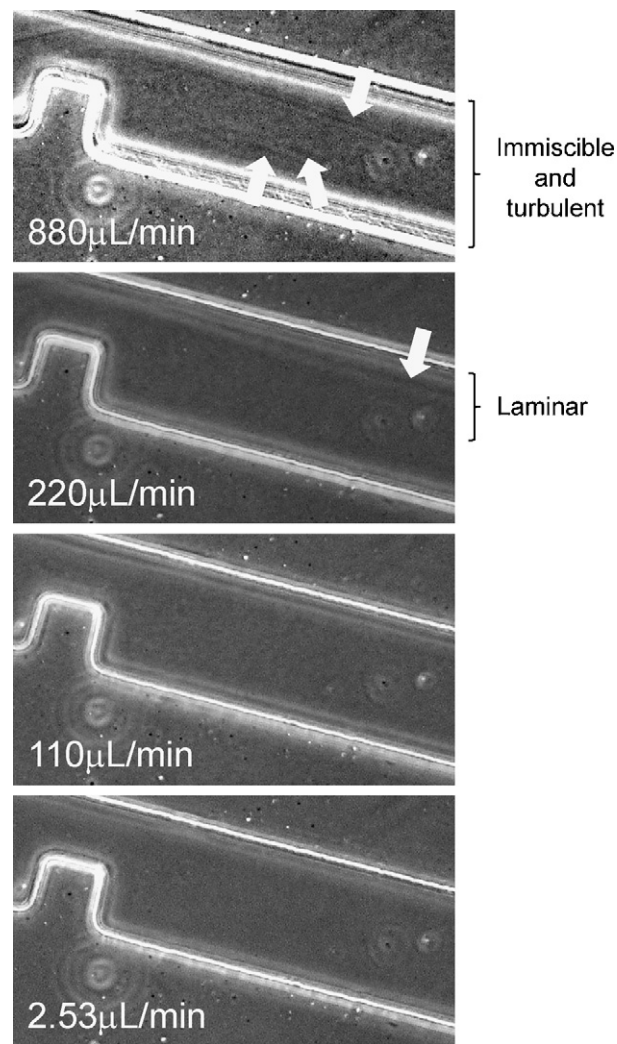


**Fig. 2.** Mixing test of micro-reactor chip by microscopy. Pictures show mixing states between 1 mg/mL ribonuclease A and  $D_2O$  at four flow rates, 2.53, 110, 220, and 880  $\mu\text{L}/\text{min}$ , in the region from zigzag to reaction area. The Picture of flow at 880  $\mu\text{L}/\text{min}$  was increased the contrast to indicate liquid-liquid interfaces clearly. White arrows indicate liquid-liquid interfaces. Flow rate at 2.53 and 110  $\mu\text{L}/\text{min}$  enough mixed two solutions, but streams at 220 and 880  $\mu\text{L}/\text{min}$  made the laminar and immiscible turbulent state, respectively.

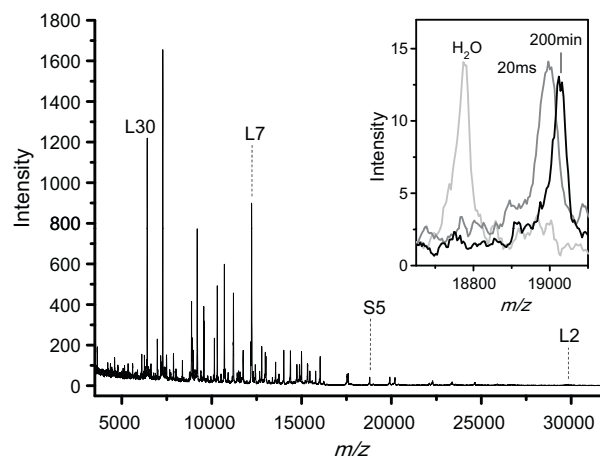


**Fig. 3.** Mass spectrum of the undeuterated ribosome. Inset shows mass spectra of S5 in  $H_2O$  and  $D_2O$ , incubated for 20 ms and 200 min.

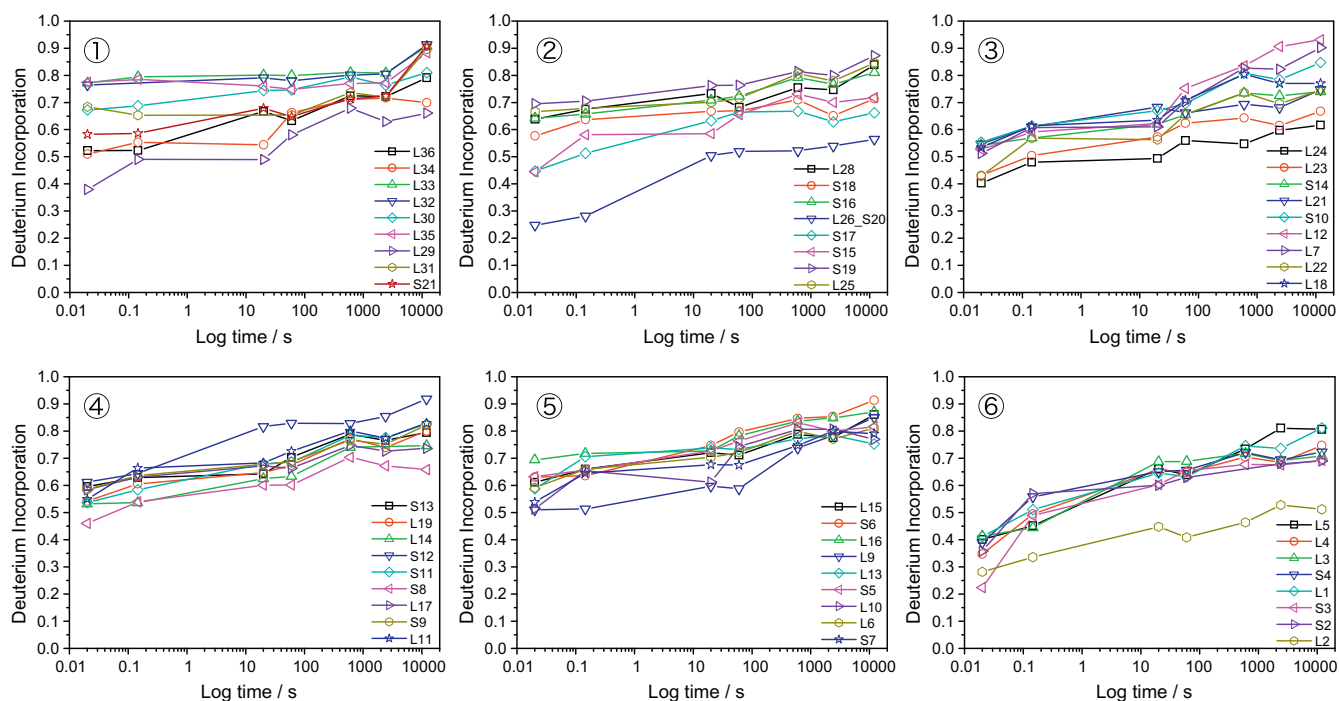


Fig. 4. Time course of deuterium incorporation into ribosomal proteins. These protein data are arranged in order of molecular weights.

To note is that sufficient deuterium incorporation occurred in all protein components at as early as 20 ms, suggesting a quality of mixing. Another important observation is that the incorporation ratio of the individual protein increased gradually as a function of time without any artificial back exchange from atmospheric  $H_2O$  that might occur if quenching procedure is eliminate. These results suggested enough efficiency of mixing and reliable quenching by the micro-reactor chip.

Variance of the HDX ratios among 52 individual proteins at 20 ms and 200 min was depicted in Fig. 5 as gray and closed columns, respectively. The open columns indicated the ratios of nonhydrogen-bonding protons on the molecular surface of each protein, that are calculated on the basis of X-ray crystallographic information of 70S ribosome [13,14].

So far as judged from the data in Fig. 4, the deuterium incorporation at 20 ms appeared to reflect conformational effects rather than primary structure effects, because extrapolation of the exchange profiles measured at later time point was not greatly deviated from the corresponding data points measured at 20 ms. However since deuterium incorporation data at earlier time points generally include both primary-structural and conformational effects under the current solvent conditions at pH 7 [15], roles of the former effect should carefully be considered in future study.

Because time scale of ribosome kinetics exists about 50 ms, the deuterium incorporation in this examination mainly depends on the movement in the time scale of a single reaction cycle for peptide elongation, including information of molecular surface. In previous study, elongation rate of peptide *in vivo* was reported as  $8\text{--}20\text{ s}^{-1}$  [16], and the elementary steps as EF-G binding and GTP hydrolysis *in vitro* have rates at  $140$  and  $250\text{ s}^{-1}$ , respectively [17–19]. Because this time scale corresponds the shorter duration than the elongation rate of peptide but longer than each elemental step, the HDX time for 20 ms means the most reasonable scale for measuring conformational changes of each elemental step. If the detection time is shorter than the elemental step, HDX would provide unclear information because of the unsynchronized movements of all molecules in solution. On the other hands, HDX data at 200 min indicates the ratio of flexible region in individual proteins. Deuterium incorpora-

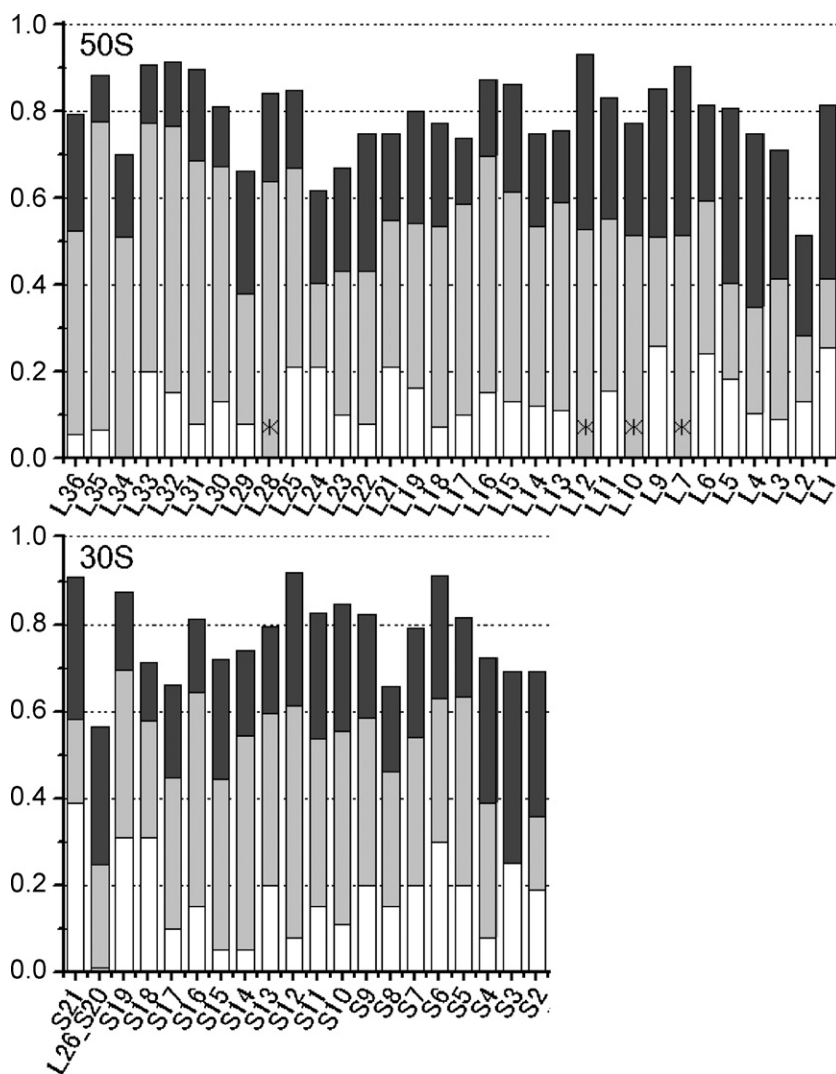
tions of all ribosomal proteins apparently completed after 200 min [8]. Strong hydrogen bonds and core region in macromolecules disallow amide group to incorporate deuterium. Therefore, the number of protected protons for 200 min shows the ratio of rigid or core structure in each protein. In Fig. 5, initiated HDX of ribosome by mixing with  $D_2O$  suggested incorporations of deuterium in the ratio from 0.00 to 0.39 (average 0.17) at once. Those proteins were deuterated in the ratio from 0.25 to 0.77 (average 0.54) at 20 ms, and from 0.56 to 0.93 (average 0.78) at 200 min. Protons finally remained at the ratio from 0.07 to 0.44 (average 0.22).

Fig. 6 show the HDX map at 20 ms and 200 min, colored each ribosomal proteins depending on the magnitude of HDX in the X-ray crystal structure [13,20]. The ribosome structure for 20 ms disallowed many deuterium to incorporate into S3, S20, and L2, which locate near the entrance of mRNA, Spur, and interface between 30S and 50S subunits, respectively. On the other hand, S6 and S12 showed higher exchange ratios for 200 min, but their mass shifts after 20 ms were normal value. The micro-reactor chip for the first time visualized individual deuterium incorporation of ribosome at the time scale comparable to a single cycle for peptide elongation, which is unavailable by pipetting.

### 3.3. The structure – movement – function relationship of ribosomal proteins

The movement of individual proteins has important roles in the structure – function relationship of a whole ribosome. Deuterium incorporations at 20 ms and 200 min provided new explanation for the relationship in this experiment. Because the HDX profile at 20 ms showed different pattern with 200 min in Fig. 5, proteins in flexible regions incorporate many deuterium at early time scale. In the time scale for 20 ms, one of the largest movements is the inter-subunit rotation in the translocation, which is carried out a few times in this time scale. Hence, it is reasonable that L2 near the axis of rotation was most protected from  $D_2O$  in all proteins of interface between subunits.

About the entrance (S12, L16, and L25), exit (L31 and L33), and frame shift region (S13) of tRNA, relative proteins in these areas



**Fig. 5.** HDX profile of ribosomal proteins. Gray and filled columns show the deuterium incorporations at 20 ms and 200 min, respectively. White columns indicate theoretical exchange ratios on the molecular surface, counted the number of nonhydrogen-bonding and exposed protons to bulk solution in X-ray structure (calculated with PDBID: 2AVY and 2AW4) [14]. \*Theoretical values of L7, L10, L12, and L28 were not counted because of disordered structures in 70S ribosome, and only L1 was calculated with 1VOR [13].

highly incorporated deuterium in both of exchange times. These HDX profile show that three binding sites of tRNA (A, P, and E sites) fluctuate functionally and have flexible structures, suggesting that the binding and recognizing of large and diverse tRNAs depend on large movements. On the other hand, S3 and S4 around the entrance of mRNA incorporated little deuterium for 20 ms (S3: 0.22 and S4: 0.39), although the exchange ratio of S4 (0.72) became the normal level at 200 min. Therefore, S4 has a standard flexibility but needs small motion at early time scale, and S3 has rigid structure at both time scales. In previous study, higher  $Mg^{2+}$  concentration stabilized ribosome structure and increased the activity of GTP hydrolysis, however S3 kept a rigid state at lower  $Mg^{2+}$  than other proteins [9]. HDX of these protein shows that the entrance of mRNA is rigid in the early time scale, predicted two unknown roles in S3; (1) unfolding of mRNA structure and (2) cleaning up ligands (small RNA chains, positive charged compounds, and metal ions etc.) on mRNA.

About the transport of nascent peptides, five proteins exist in the tunnel (L4 and L22) and exit (L23, L24, and L29). Proteins around the exit incorporated little deuterium at both exchange time, while L4 and L22 in tunnel was little at only 20 ms. From HDX experiment for 200 min, The tunnel are possible to pass nascent peptides having various sizes and polarities without the clogging by the flex-

ibility. Then, the L23, L24, and L29 behave as the rigid structure, although the exit hole enough contact with bulk solution. On the other hand, tunnel and exit proteins incorporated little deuterium at 20 ms (L4: 0.35, L22: 0.43, L23: 0.43, L24: 0.40, and L29: 0.38), although nascent peptides dynamically move near them. Therefore HDX profile and map show that nascent peptides get the driving force of the transport from others.

L7/L12, L11, and L1 as stalk proteins were predicted to incorporate many deuterium at 20 ms, because static structures showed disordering of the electron density by X-ray crystallography. However, HDX of stalk proteins were normal or lower level in early time scale, incorporated many deuterium at 200 min. Therefore, the movement of these proteins may spend a long time over 20 ms and/or need trigger such as ligand binding.

About the other proteins of 30S subunit, the rigid structure exist in area among the platform, body, and spur, because S8, S15, S17, and S20 incorporated little deuterium for both 20 ms and 200 min (Fig. 6). In, addition, these proteins are also known as contributors to structural formation in the primary stages of assembly [21–23]. These evidences mean that the basis of 30S subunit structure formed around this area, and four proteins are casted in the stabilizer of 16S rRNA. On the other hand, the neck area consist

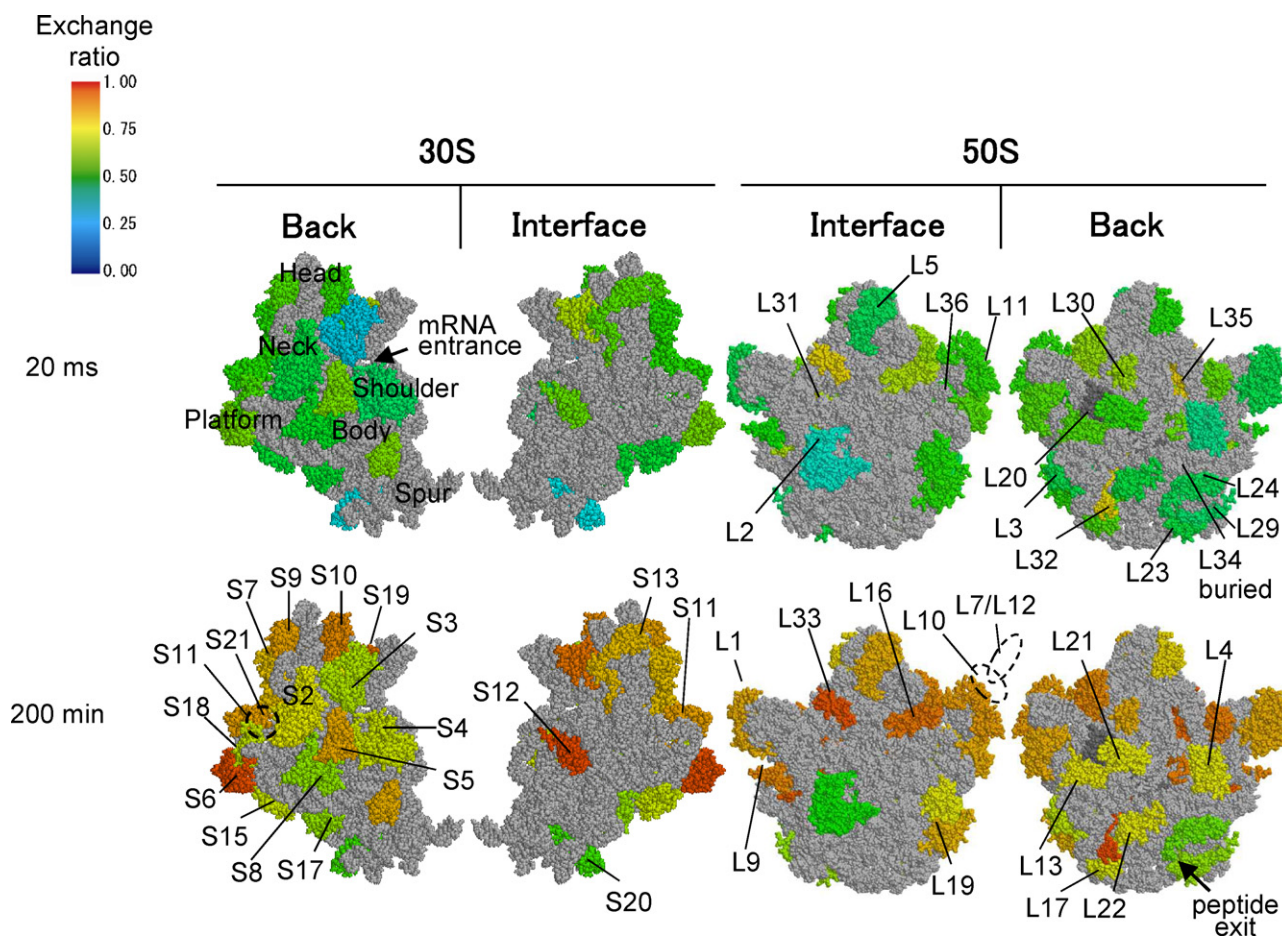


**Fig. 6.** HDX map for ribosomal proteins at 20 ms and 200 min (PDBID: 1PNS and 1VOR) [13,20]. Light gray indicates rRNA molecules and the color of each proteins depends on the magnitude of deuterium incorporations. Dotted circles show positions of L7/L12, L10 and S21.

of some proteins and the thin RNA, connecting head and other area. Therefore, the head domain is controlled the range and rate of the movement by the neck area. S2 located on rRNA in the area from head to platform. If head and platform moved independently, S2 should incorporate many deuterium. S2 incorporated little deuterium for 20 ms, although the ratio became normal level at 200 min. These HDX data suggest a new role in S2, which works as a brace between head and platform area.

#### 4. Conclusion

Here we designed a micro-reactor chip which enables us to demonstrate HDX with high temporal resolution. This chip device has the performance of rapid quenching at  $20.1 \pm 2.7$  ms, detecting structural changes of 52 ribosomal proteins in solution at the time scale comparable to a single reaction cycle for the peptide elongation. The comparison of HDX profile and the map at 20 ms and 200 min elucidated novel characteristic behavior of individual proteins of ribosome in solution. The data in the different time scale suggested that the localization of protein movement plays important roles in the peptide elongation and complex stability. In future work, rapid quenching HDX of reaction intermediates using the current micro-reactor chip technique will progress the definite elucidation for structure – function relationship of ribosome and other macromolecular complexes.

Refinement of design of the micro-reactor chip will help us achieve greater time resolution for rapid quenching that enables us to analyze structural changes involving individual reaction steps by rearranging the shape of flow paths and solvent conditions.

Development of the HDX analyses with sub-millisecond resolution deserves further efforts, provided that collection of the data from such analyses provided direct evidence for molecular dynamics simulation of various macromolecular complexes using supercomputer.

#### Acknowledgements

We thank Dr. Koji Takio (RIKEN) and Dr. Noriyasu Oshima (Gunma Univ.) for experimental advices and supports. This work was supported by JST, ERATO, Suematsu Gas Biology Project (at Keio University School of Medicine), Tokyo 160-8582, Japan. The structure-function relationship study on ribosome was assisted by a Grant-in-Aid for Young Scientist (B) No.20770129 from the Ministry of Education, Culture, Sports Science and Technology of Japan. MS is also supported by Research and Development of the Next- Generation Integrated Simulation of Living Matter, a part of the Development and Use of the Next-Generation Supercomputer Project of MEXT.

#### References

- [1] Z. Zhang, D.L. Smith, Determination of amide hydrogen exchange by mass spectrometry: a new tool for protein structure elucidation, *Protein Sci.* 2 (1993) 522–531.
- [2] T. Yamamoto, S. Izumi, K. Gekko, Mass spectrometry on hydrogen/deuterium exchange of dihydrofolate reductase: effects of ligand binding, *J. Biochem.* 135 (2004) 663–671.
- [3] T. Yamamoto, S. Izumi, E. Ohmae, K. Gekko, Mass spectrometry of hydrogen/deuterium exchange of *Escherichia coli* dihydrofolate reductase: effects of loop mutations, *J. Biochem.* 135 (2004) 487–494.

- [4] N. Ban, P. Nissen, J. Hansen, P.B. Moore, T.A. Steitz, The complete atomic structure of the large ribosomal subunit at 2.4 Å resolution, *Science* 289 (2000) 905–920.
- [5] B.T. Wimberly, D.E. Brodersen, W.M. Clemons Jr., R.J. Morgan-Warren, A.P. Carter, C. Vonrhein, T. Hartsch, V. Ramakrishnan, Structure of the 30S ribosomal subunit, *Nature* 407 (2000) 327–339.
- [6] M. Valle, A. Zavialov, J. Sengupta, U. Rawat, M. Ehrenberg, J. Frank, Locking and unlocking of ribosomal motions, *Cell* 114 (2003) 123–134.
- [7] W. Zhang, J.A. Dunkle, J.H. Cate, Structures of the ribosome in intermediate states of ratcheting, *Science* 325 (2009) 1014–1017.
- [8] T. Yamamoto, S. Izumi, K. Gekko, Mass spectrometry of hydrogen/deuterium exchange in 70S ribosomal proteins from *E. coli*, *FEBS Lett.* 580 (2006) 3638–3642.
- [9] T. Yamamoto, Y. Shimizu, T. Ueda, Y. Shiro, Mg<sup>2+</sup> dependence of 70 S ribosomal protein flexibility revealed by hydrogen/deuterium exchange and mass spectrometry, *J. Biol. Chem.* 285 (2010) 5646–5652.
- [10] D.A. Simmons, S.D. Dunn, L. Konermann, Conformational dynamics of partially denatured myoglobin studied by time-resolved electrospray mass spectrometry with online hydrogen-deuterium exchange, *Biochemistry* 42 (2003) 5896–5905.
- [11] P. Liuni, T. Rob, D.J. Wilson, A microfluidic reactor for rapid, low-pressure proteolysis with on-chip electrospray ionization, *Rapid Commun. Mass Spectrom.* 24 (2010) 315–320.
- [12] H. Ohashi, Y. Shimizu, B.W. Ying, T. Ueda, Efficient protein selection based on ribosome display system with purified components, *Biochem. Biophys. Res. Commun.* 352 (2007) 270–276.
- [13] A. Vila-Sanjurjo, B.S. Schuwirth, C.W. Hau, J.H. Cate, Structural basis for the control of translation initiation during stress, *Nat. Struct. Mol. Biol.* 11 (2004) 1054–1059.
- [14] B.S. Schuwirth, M.A. Borovinskaya, C.W. Hau, W. Zhang, A. Vila-Sanjurjo, J.M. Holton, J.H. Cate, Structures of the bacterial ribosome at 3.5 Å resolution, *Science* 310 (2005) 827–834.
- [15] Y. Bai, J.S. Milne, L. Mayne, S.W. Englander, Primary structure effects on peptide group hydrogen exchange, *Proteins* 17 (1993) 75–86.
- [16] R. Young, H. Bremer, Polypeptide-chain-elongation rate in *Escherichia coli* B/r as a function of growth rate, *Biochem. J.* 160 (1976) 185–194.
- [17] A. Savelsbergh, V.I. Katunin, D. Mohr, F. Peske, M.V. Rodnina, W. Wintermeyer, An elongation factor G-induced ribosome rearrangement precedes tRNA-mRNA translocation, *Mol. Cell.* 11 (2003) 1517–1523.
- [18] E.G. Wagner, P.C. Jelenc, M. Ehrenberg, C.G. Kurland, Rate of elongation of polyphenylalanine in vitro, *Eur. J. Biochem.* 122 (1982) 193–197.
- [19] T. Ruusala, M. Ehrenberg, C.G. Kurland, Is there proofreading during polypeptide synthesis? *EMBO J.* 1 (1982) 741–745.
- [20] A. Vila-Sanjurjo, W.K. Ridgeway, V. Seymaner, W. Zhang, S. Santoso, K. Yu, J.H. Cate, X-ray crystal structures of the WT and a hyper-accurate ribosome from *Escherichia coli*, *Proc. Natl. Acad. Sci. USA* 100 (2003) 8682–8687.
- [21] S. Mizushima, M. Nomura, Assembly mapping of 30S ribosomal proteins from *E. coli*, *Nature* 226 (1970) 1214–1218.
- [22] M.I. Recht, J.R. Williamson, RNA tertiary structure and cooperative assembly of a large ribonucleoprotein complex, *J. Mol. Biol.* 344 (2004) 395–407.
- [23] J.F. Gronddek, G.M. Culver, Assembly of the 30S ribosomal subunit: positioning ribosomal protein S13 in the S7 assembly branch, *RNA* 10 (2004) 1861–1866.